

XI-11. Ultrasonic Amplification and Non-Ohmic Behavior in Tellurium

T. ISHIGURO* and T. TANAKA

*Department of Electronics, Faculty of Engineering,
 Kyoto University, Kyoto, Japan*

A transverse ultrasonic wave of 45 Mc/sec propagating along the y axis in p -type tellurium was amplified in a strong electric field at 77°K. The characteristics of amplification are found to be described by White's theory. Comparison of the experiment with the theory enables one to obtain the value of a piezoelectric constant, $e_{11}=0.6\text{ C/m}^2$. Critical drift velocities of holes observed at the onset of non-ohmic conduction along three crystallographic axes are in rather good agreement with the velocities of elastic waves.

§ 1. Introduction

It is well known that piezoelectricity is observed in II-VI and III-V compound semiconductors which have ionic bonds. Elemental semiconductors such as Te and Se are also piezoelectric,¹⁾ though the physical basis of piezoelectricity of them has not been revealed so far.

Hutson *et al.* and White²⁾ have shown the possibility of ultrasonic travelling-wave amplification in any piezoelectric semiconductors. It is expected, therefore, that the ultrasonic wave may be amplified in Te and Se. At present it is very difficult to amplify ultrasonic waves in Se, because of the small mobility of carriers ($\mu \sim 1\text{ cm}^2/\text{V sec}$) and the difficulty of preparation of large single crystals. For Te, one need not worry about such difficulties. In fact, the related phenomena such as current saturation and current instability in Te have been already observed by G. Quentin *et al.*³⁾ and the present authors.⁴⁾

According to White's theory,²⁾ a plane elastic wave in a piezoelectric semiconductor may couple with drifting carriers when it accompanies a longitudinal electric field. Table I shows the calculated phase velocities of sounds propagating along three principal crystallographic axes in Te and whether the sound may couple with carriers or not. Only the longitudinal wave propagating along the x axis and the transverse wave propagating along the y axis are expected to couple with carriers and hence to be amplified.

§ 2. Ultrasonic Amplification

Single crystals Te were prepared by the Czochralski method using 99.9999% Te. The sample was cut by cleavage from the crystal which was pulled up along the y axis. The lateral faces of the sample were etched to prepare the cylindrical sample. The cross-section of the sample was 42 mm^2 and the length was 3.9 mm. Ni was plated as electrodes, on which Au

Table I. Summary of calculated sound velocities and coupling with carriers along three crystallographic axes.

Propagating direction	Vibrating mode	Sound velocity* V_s (m/sec)	Coupling through piezoelectricity
x axis	Longitudinal	2410	Yes
	Transverse-1	2570	No
	Transverse-2	1040	No
y axis	Transverse	1470	Yes
	Quasi-longitudinal	2810	No
	Quasi-transverse	1850	No
z axis	Longitudinal	3590	No
	Transverse (degenerated)	2350	No

* Calculated from the elastic constants presented in ref. 6).

* Present address: Electrotechnical Laboratory, Tanashi, Tokyo.

was evaporated to reduce the resistance of the electrodes of large area. A y -cut quartz transducer was cemented on the suitable position of a electrode with Canada balsam (Fig. 1), considering that the direction of energy flux is not

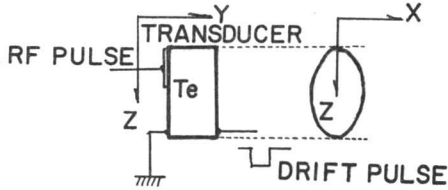


Fig. 1. Experimental arrangement.

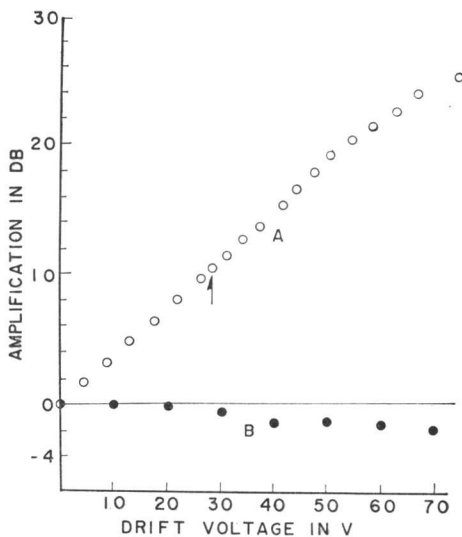


Fig. 2. Observed ultrasonic amplification as a function of drift voltage. Zero dB represents the attenuation in the sample at no electric field. A: relative amplitude of echoes of transverse wave, B: that of quasi-transverse wave.

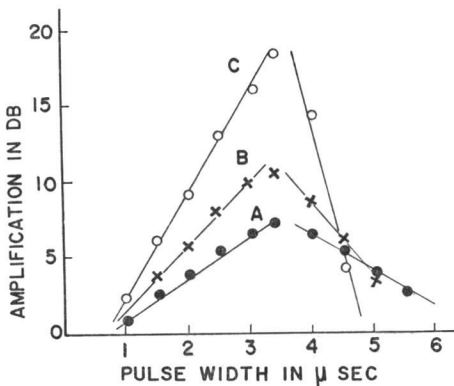


Fig. 3. Observed ultrasonic travelling-wave amplification as a function of width of drift pulse. A: drift pulse of 18 V, B: drift pulse of 28 V, C: drift pulse of 53 V.

parallel to the normal of the wave front of transverse wave propagating along the y axis.

The sample was cooled to $77^\circ K$, where the conduction was p -type and the conductivity was $\sigma_{11} = 2.7 \times 10^{-2} / \Omega cm$. The ultrasonic wave of 45 Mc/sec was generated and detected with a y -cut quartz transducer. The voltage pulse was applied to drift holes in the direction of propagation of the sound.

Figure 2 shows the relative amplitudes of detected echoes of transverse wave and quasi-transverse wave versus applied electric field. Zero dB of the vertical axis indicates the amplitude of echo detected under the condition of no applied electric field. The arrow indicates the voltage of drift pulse at the onset of non-ohmic characteristics, where the drift velocity of holes became equal to the sound velocity as will be described later. The amplitudes of echoes of transverse wave increased exponentially with the applied electric field but those of quasi-transverse wave were rather independent of the applied field.

The amplitudes of echoes of transverse wave also depended on the width of the applied drift pulse as shown in Fig. 3. The amplitude increased exponentially until the critical value of pulse width corresponding to the transit time of sound, but decreased rapidly beyond the critical value.

According to White's small signal theory²⁾ which is valid under the condition of $kl < 1$, where k is the wave number of the sound and l is the mean free path of carriers, the attenuation constant α in neper/cm of sound in piezoelectric semiconductors is expressed by

$$\alpha = \frac{1}{2} \frac{e^2}{\epsilon c} \frac{\omega_e}{V_s \gamma} \left\{ 1 + \frac{\omega_e^2}{\gamma^2 \omega^2} \left(1 + \frac{\omega^2}{\omega_e \omega_D} \right)^2 \right\}^{-1}$$

$$\gamma = 1 - \frac{\mu E}{V_s}, \quad (1)$$

where e is the piezoelectric constant, ϵ is the dielectric constant, c is the elastic constant, $\omega_e = \sigma/\epsilon$ is the dielectric relaxation frequency, $\omega_D = V_s^2/D$ is the diffusion frequency, D is the diffusion constant, E is the applied electric field, and ω and V_s are the frequency and the velocity of the sound, respectively.

In case of the transverse wave propagating in the direction of the y -axis in Te, e , ϵ and c are replaced by e_{11} , ϵ_{11} and c_{66} , respectively. Since $\omega_e \cong 10^{10}$ c/sec $\omega_D \cong 10^9$ c/sec and $\omega \cong 3 \times 10^8$ c/sec in our case, eq. (1) is simplified as,

$$\alpha = \frac{1}{2} \frac{e_{11}^2}{c_{66}} \frac{\omega^2}{V_s \sigma_{11}} \left(1 - \frac{\mu E}{V_s} \right). \quad (2)$$

To compare the theory with the experimental result, it is convenient to modify the equation so as to give $\alpha=0$ when $E=0$, *ie.*,

$$\alpha - \alpha_{E=0} = -4.34 \frac{e_{11}^2}{c_{66}} \frac{\omega^2}{V_s \sigma_{11}} \frac{\mu E}{V_s} \quad dB/cm, \quad (3)$$

where $\alpha - \alpha_{E=0}$ gives the apparent attenuation by drifting carriers. Comparing eq. (3) with the experiment (Fig. 2), we have

$$4.34 \frac{e_{11}^2}{c_{66}} \frac{\omega^2}{V_s \sigma_{11}} = 27 \quad dB/cm,$$

where it is assumed that $\mu E = V_s$ at the onset of non-ohmic conduction. If we use the values: $\omega = 2.38 \times 10^8$ c/sec, $V_s = 1.47 \times 10^5$ cm/sec, $c_{66} = 1.36 \times 10^{11}$ dyne/cm²,⁶⁾ $\sigma_{11} = 2.7 \times 10^{-2}/\Omega$ cm, then we obtain $e_{11} = 0.6$ C/m². Here, it should be remarked that the piezoelectric constants of high conductive materials may be determined from the experiment of ultrasonic amplification in the same way as shown in this case.

The gradient of the curve in Fig. 3 gives the attenuation constant $\alpha - \alpha_{E=0}$ in dB/cm, since pulse width is proportional to the distance interacting with drifting carriers. According to eq. (3), the gradients before and after the reverse of the travelling direction of sound are expected to be equal, *ie.*,

$$|\alpha_{E=E_d} - \alpha_{E=0}| = |\alpha_{E=-E_d} - \alpha_{E=0}|, \quad (4)$$

where E_d is the applied field. The experimental results show that the gradient after reflection is larger than that before reflection. The increase of attenuation constant may be attributed to the interaction with the ultrasonic flux generated spontaneously, which propagates in the opposite direction to the sound echo. One fact which supports our explanation is seen in Fig. 3: The deviation from eq. (4) becomes larger as the drift voltage increases.

In principle it is possible to amplify the longitudinal wave propagating along the x axis. The amplification factor, however, is diminished by a factor of 1/4.6 compared to the transverse wave along the y axis because of the larger values of V_s and c_{ij} . The other waves which propagate along the direction of non-principal axes of crystal may be also amplified, but those modes are too complicated to be detected practically.

§ 3. Non-Ohmic Behavior—Anisotropy

When the applied electric field becomes larger than a critical value (E_c) in Te, non-ohmic behavior begins to appear. The samples oriented to one of the crystallographic axes were prepared in the shape of bar of cross-section 5~10 mm² and length 8~14 mm. The non-ohmic V-I characteristics were observed in any sample, not only in the samples parallel to the x and y axes, but also in the samples parallel to z axis as shown in Fig. 4. In the former case carriers drifting along the axis of the sample may couple with sounds, while in the latter case carriers cannot couple with sound through longitudinal electric field as shown in Table I.

The drift velocities of holes V_{dc} at the onset of non-ohmic conduction estimated from the values of E_c and Hall mobility μ_H are summarized in Table II for three crystallographic axes. The values of V_{dc} in the direction of x and y axes are in rather good agreement with the velocity of elastic wave which may couple with carriers. The discrepancy between V_{dc} of Table

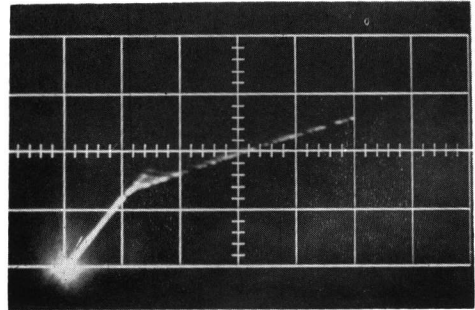


Fig. 4. Drift current vs. drift voltage in Te sample parallel to z axis (Cz 712). Vertical scale: 0.35 A/div., horizontal scale: 74 V/div. .

Table II. Summary of V_{dc} data for three crystallographic axes.

	Hall mobility of holes μ_H (cm ² /Vsec)	Critical field E_c (V/cm)	Drift velocity of holes V_{dc} (m/sec)
x axis			
Cx 603	1670	104	1740
Cx 103	1430	150	2150
Cx 104	2060	114	2350
y axis			
Cy 102	2560	54	1380
Cy 105	2540	73	1850
Cy 106	2200	73	1600
Cy 107	1680	80	1340
z axis			
Cz 712	3160	76	2390
Cz 101	5020	51	2550

II and V_s of Table I may be caused by the ambiguity of the values of E_c (+10~−15%) and by the difference between drift and Hall mobilities.

On the other hand at the onset of non-ohmic behavior in the sample along the z axis, the drift velocity of carriers correspond to the velocity of transverse wave which cannot couple with carriers through longitudinal electric field. To explain the difference between the critical drift velocities and the sound velocity which may couple with carriers in CdS, McFee⁷⁾ put forward the following hypothesis: The departure from ohmic behavior are brought about by the amplification of waves whose wave vectors make finite angle with the current direction. Such mechanism, however, is not expected in Te, because any sound cannot be the cause of the potential fluctuation along the z axis through piezoelectricity from the view point of crystal symmetry. Moreover, in our case the samples parallel to the z axis were rightly oriented, because they were cut from the crystal by cleavage. The origin of the non-ohmic behavior in the sample parallel to the z axis is therefore ambiguous at present.

DISCUSSION

Pustovoit, V.I.: Could you tell me whether it was possible in your experiments to get a stationary regime? I mean to use a dc electric field but not a pulse one.

Ishiguro, T.: Ultrasonic amplification in Te under dc electric field is impossible, because the sample is highly conductive and is heated by Joule heat.

Pustovoit, V.I.: You have noticed that CdS is a poor material for amplification of sound waves because it has a small mobility. I would like to point out that in our experiments we managed to obtain a dc field amplification of transverse sound wave in CdSe at room temperature. The wave frequency was 400 Mc and the amplification was approximately 60 dB/cm. In addition we investigated the acousto-electric effect in CdSe as a function of dc electric field strength. Experimental data are in good agreement with theory.

Inuishi, Y.: Does your amplification factor α depend on the conductivity of the sample?

Ishiguro, T.: Yes. But precisely speaking it depends on the carrier concentration,

$$\alpha \text{ apparent} \propto \mu/\sigma = 1/en.$$

Neuringer, L.J.: Are your results concerning the amplification reproducible after repeated cycling between room temperature and 77°K?

Ishiguro, T.: Yes, they are.

Acknowledgements

The authors would like to express their thanks to Prof. A. Aoyagi of Osaka University and Prof. A. Kawabata of Kyoto University for their encouragement. They are indebted to Dr. N. Mikoshiba of Electrotechnical Laboratory for his helpful discussions. They also would like to express their thanks Mr. A. Hotta and Mr. S. Nitta for their supports in the experimental work.

References

- 1) H. Gobrecht, H. Hamisch and A. Tausend: *Z. Phys.* **148** (1957) 209; G. Quentin and J. M. Thuillier: *Solid State Commun.* **2** (1964) 115.
- 2) A. R. Hutson and D. L. White: *J. appl. Phys.* **33** (1962) 40; D. L. White: *J. appl. Phys.* **33** (1962) 2547.
- 3) G. Quentin and J. M. Thuillier: *Proc. Int. Conf. Semiconductor Physics*, Paris (1964) p. 571.
- 4) T. Ishiguro, S. Nitta, A. Hotta and T. Tanaka: *Japan. J. appl. Phys.* **4** (1965) 703.
- 5) P. C. Waterman: *Phys. Rev.* **113** (1959) 1240.
- 6) J. L. Malgrange, G. Quentin and J. M. Thuillier: *Phys. Status solidi* **4** (1964) 139.
- 7) J. H. McFee: *J. appl. Phys.* **34** (1963) 1548.